Georgian Mathematical Journal
Volume 14 (2007), Number 1, 109–122

NEAR FIELD REPRESENTATIONS OF THE ACOUSTIC GREEN'S FUNCTION IN A SHALLOW OCEAN WITH FLUID-LIKE SEABED

ROBERT GILBERT AND MIAO-JUNG OU

Abstract. In this paper, the near-field approximation of the acoustic Green's function in a two-layer waveguide is constructed by using a variation of the method of Ahluwalia and Keller [1]. The relation between the constructed multiple-scattering representation (suitable for near-field) and the Hankel transform representation (suitable for mid-range) is also discussed in this paper. The construction scheme presented in this paper can be generalized for an N-layer waveguide.

2000 Mathematics Subject Classification: 34E05, 35A35, 35G15, 35J05, 41A60, 74H10.
Key words and phrases: Layered waveguide, acoustic Green's function, Helmholtz equation, near-field approximation, multiple-scattering representation.

1. Introduction

In this paper, we show how to construct acoustic Green's functions for a water column with fluid-like basement atop a rigid rockbed. The main interest is to obtain a representation of the acoustic Green's function which is valid in the near field. It is hoped with a near field Green's function, we will be able to solve the unknown object, inverse problem for an object submerged in an ocean with a layer of fluid-like sediment atop rigid rock, much in the same way as in [5], [3] for the completely reflecting seabed. In these papers, the method of integral equations is used, hence the need for an accurate near-field approximation. An alternate method which could also make use of an accurate near-field Green's function is the method of complete families of solutions. The idea of this method is discussed in [2] by Bergman and Schiffer, but goes back much farther. This method has been used effectively by Angell, Kleinman, Lesselier, and Rozier [6, 7] who used the fact that the Green's function evaluated on a dense set of points in the interior of the bounding curve of the unknown object provides a complete family [2].

Our approach makes use of an idea put forth in a paper by Ahluwalia and Keller [1]. Their method generalizes the method of images representation of the Green's function for a homogeneous shallow ocean with reflecting seabed with

ISSN 1072-947X / \$8.00 / © Heldermann Verlag *www.heldermann.de*

finite depth h, namely

$$G(\mathbf{x}, \mathbf{x}_0) = \sum_{n=-\infty}^{\infty} (-1)^n \left(\frac{e^{ik\sqrt{(x-x_0)^2+(y-y_0)^2+(z-z_0+2nh)^2}}}{\sqrt{(x-x_0)^2+(y-y_0)^2+(z-z_0+2nh)^2}} - \frac{e^{ik\sqrt{(x-x_0)^2+(y-y_0)^2+(z+z_0+2nh)^2}}}{\sqrt{(x-x_0)^2+(y-y_0)^2+(z+z_0+2nh)^2}} \right),$$

where (x_0, y_0, z_0) is the source location and k is the wave number, which is defined as the ratio of acoustic frequency and the acoustic wave speed in the ocean. This representation is called the ray representation of the Green's function. This method can be further generalized to a stratified ocean and the resulting representation is called the multiple scattering expansion of the Green's function [1]. Although it is well known that the ray/multiple scattering representation is mathematically equivalent to the modal expansion [1], actual computations with each of these representations can return different results due to truncation errors. This is especially true for the two extreme cases, i.e. when the point of measurement is very close to or far away from the acoustic source point.

We are interested in the model of an ocean with a fluid-like seabed. It is modeled as a two-layered waveguide. Within each layer, the acoustic property can be smoothly varied with respect to depth. On the interface between the two layers, there is a jump in the refractive index $n(z) := c(z)/c_0$ and continuity of acoustic displacement and acoustic pressure are imposed there as transmission conditions. The modal expansion of the Green's function for a waveguide of two homogeneous layers is already given in ([4]). In this paper, we construct the multiple scattering expansion of the Green's function. The relation between the modal expansion and the multiple scattering expansion of the Green's function is also discussed.

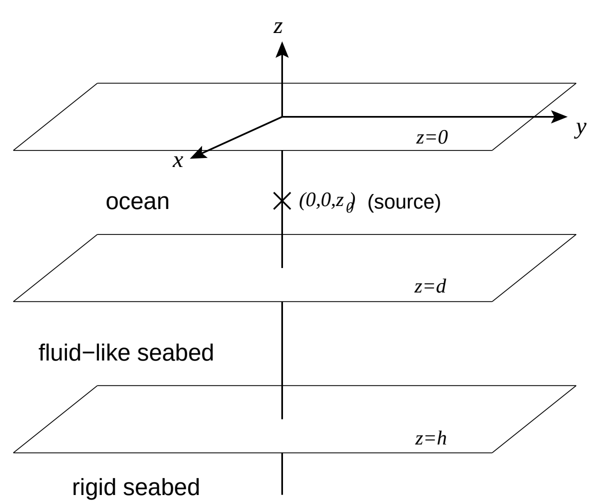

FIGURE 1. Schematic description of the Pekeris waveguide

1.1. **Construction of the near-field representation of the Green's function.** We consider a waveguide, which consists of a finite, uniform depth water column lying over a fluid-like seabed as shown in Figure 1. The waveguide can be stratified, i.e. the acoustic property is not necessarily homogeneous in each layer.

We shall use the subscript 1 for the material parameters in the water column and the subscript 2 for those in the basement; whereas for the ease of notation, we will use $p^{(1)}$ and $p^{(2)}$ to denote the acoustic pressure in the ocean and the seabed, respectively. Moreover, we assume that the acoustic source is situated in the water column at $r = 0$ and $z = z_0$ in cylindrical coordinates. Hence, in the water column, the time harmonic acoustic pressure $p^{(1)}$ must satisfy the nonhomogeneous Helmholtz equation

$$\Delta p^{(1)} + k^2 n_1(z)\, p^{(1)} = -\delta(z - z_0)\frac{\delta(r)}{2\pi r}. \tag{1}$$

In the fluid-like sediment, the acoustic pressure $p^{(2)}$ satisfies the homogeneous Helmholtz equation

$$\Delta p^{(2)} + k^2 n_2(z)\, p^{(2)} = 0, \tag{2}$$

where k is a constant defined as $k := \frac{\omega}{c_0}$ with ω being the frequency of acoustic waves and c_0 the reference sound speed. The refractive index function $n_i(z)$ in the layer i, $i = 1, 2$, is the ratio of the reference sound speed c_0 and the sound speed function $c_i(z)$, which is assumed to be continuous within each layer.

At the ocean surface there is a pressure release boundary condition,

$$p^{(1)} = 0 \text{ at } z = 0. \tag{3}$$

Across the two-fluid interface $z = d(< 0)$, two transmission conditions are required such that the normal component of particle velocity and acoustic pressure be preserved,

$$\lim_{z\to d^+} \frac{1}{\rho_1}\frac{\partial p^{(1)}}{\partial z}(x, y, z) = \lim_{z\to d^-} \frac{1}{\rho_2}\frac{\partial p^{(2)}}{\partial z}(x, y, z), \tag{4}$$

$$\lim_{z\to d^+} p^{(1)}(x, y, z) = \lim_{z\to d^-} p^{(2)}(x, y, z). \tag{5}$$

At the bottom $z = h(< 0)$, the complete reflecting condition reads as

$$\frac{\partial p^{(2)}}{\partial z} = 0 \text{ at } z = h. \tag{6}$$

It is convenient to use the Hankel transform

$$\tilde{p}(ka, z) := 2\pi \int_0^\infty J_0(kar)\, p(r, z)\, r\, dr$$

to reduce the dimensionality of our problem, where J_0 is the Bessel function of order zero. Imposing the out-going radiation conditions on p and applying the

Hankel transformation to equations (1)–(6) lead to the following system:

$$\frac{\partial^2}{\partial z^2}\tilde{p}^{(1)}(ka,z) + k^2\left(n_1(z)^2 - a^2\right)\tilde{p}^{(1)}(ka,z) = -\delta\left(z - z_0\right), \quad d < z < 0, \tag{7}$$

$$\frac{\partial^2}{\partial z^2}\tilde{p}^{(2)}(ka,z) + k^2\left(n_2(z)^2 - a^2\right)\tilde{p}^{(2)}(ka,z) = 0, \quad h < z < d, \tag{8}$$

$$\tilde{p}^{(1)}\left(ka,0\right) = 0, \tag{9}$$

$$\lim_{z\to d^+}\frac{1}{\rho_1}\frac{\partial\tilde{p}^{(1)}}{\partial z} = \lim_{z\to d^-}\frac{1}{\rho_2}\frac{\partial\tilde{p}^{(2)}}{\partial z}, \tag{10}$$

$$\lim_{z\to d^+}\tilde{p}^{(1)} = \lim_{z\to d^-}\tilde{p}^{(2)}, \tag{11}$$

$$\frac{\partial\tilde{p}^{(2)}}{\partial z}\left(h\right) = 0. \tag{12}$$

For the ease of notation, we define $f(c^+)$ and $f(c^-)$ as

$$f(c^+) := \lim_{z\to c^+} f(z)$$

$$f(c^-) := \lim_{z\to c^-} f(z)$$

for any given function $f(z)$ and fixed number c. This notation will be extensively used in the rest of the paper.

2. The Method of Ahluwalia and Keller

To demonstrate the singular behavior of the Green's function, we apply a variation on the method of images suggested in [1] for a completely reflecting seabed. To this end, we seek for the Hankel transform of the Green's function $G(r,z;0,z_0)$ as a multiple scattering representation in the form

$$G(r,z;0,z_0) = \sum_{n=0}^{\infty} \psi_n(r,z).$$

Here $\psi_0(r,z)$ represents a direct wave from the source at $(0,z_0)$; $\psi_1(r,z)$ represents a wave which has been either reflected or refracted once, and $\psi_n(r,z)$ is a wave which has gone through n such actions. A particular nicety of this method is that the refractive index function n_j, $j = 1, 2$, can vary with respect to z.

For convenience, we work with the Hankel-transformed system (7)$\sim$(12). In order to construct the scattered waves we need two linearly independent solutions of the homogeneous form of (7). Let us designate these two solutions in the water column as $U^{(1)}(ka,z)$ and $D^{(1)}(ka,z)$ as up-going and down-going solutions respectively, relative to z_0. We normalize these solutions such that their Wronskian at $z = z_0$ is $-2ik$. Similarly, $U^{(2)}(ka,z)$ and $D^{(2)}(ka,z)$ are two linearly independent solutions of (8).

In terms of the convention

$$z_> := \max\{z, z_0\}, z_< := \min\{z, z_0\},$$

the first term in the multiple scattering representation is seen to be

$$\tilde{\psi}_0(ka, z) = \begin{cases} \dfrac{U^{(1)}(ka, z_>)\ D^{(1)}(ka, z_<)}{-2ik}, & d < z < 0, \\ 0 \qquad\qquad\qquad\qquad\qquad\quad , & h < z < d. \end{cases}$$

Obviously $\tilde{\psi}_0$ satisfies (7).

To simplify the notation, we will hereafter omit the variable ka in $U^{(1)}(ka, z)$, $D^{(1)}(ka, z)$, $U^{(2)}(ka, z)$ and $D^{(2)}(ka, z)$.

To calculate the next term in this representation we proceed as follows. When $\tilde{\psi}_0$ is incident upon the water column surface at $z = 0$, it produces a down-going wave. Since $U^{(1)}$ and $D^{(1)}$ are linearly independent solutions to a second-order linear ordinary differential equation, this downward wave must be proportional to $D^{(1)}(z)$. For convenience, we write it in the form

$$R_1\ D^{(1)}(z_0)\ D^{(1)}(z)/(-2ik)\,,$$

where R_1 is referred to as the reflection coefficient of the water surface. To compute R_1, we use the boundary condition at the surface $z = 0$,

$$\tilde{\psi}_0(ka, 0) + \frac{R_1\ D^{(1)}(ka, z_0)\ D^{(1)}(0)}{-2ik} = 0\,,$$

which implies

$$R_1 = -\frac{U^{(1)}(0)}{D^{(1)}(0)}\,. \tag{13}$$

Similarly, as $\tilde{\psi}_0$ is incident upon the interface $z = d$, it produces an up-going wave in the water column and a down-going wave in the fluid-like seabed. We denote the first one by $R_2U^{(1)}(z_0)U^{(1)}(z)/(-2ik)$ and the second one by $T_1U^{(1)}(z_0)D^{(2)}(z)/(-2ik)$, where R_2 is referred to as the reflection coefficient and T_1 as the transmission coefficient on the interface. To calculate these coefficients, we apply (11) and (10) to obtain

$$\begin{aligned} &\tilde{\psi}_0(ka, d^+) + \frac{R_2U^{(1)}(z_0)U^{(1)}(d^+)}{-2ik} \\ &= \frac{T_1U^{(1)}(z_0)D^{(2)}(d^-)}{-2ik} \\ &\left(\frac{1}{\rho_1}\frac{\partial\tilde{\psi}_0}{\partial z}\right)(ka, d^+) + \frac{R_2U^{(1)}(z_0)}{-2ik}\left(\frac{1}{\rho_1}\frac{\partial U^{(1)}}{\partial z}\right)(d^+) \\ &= \frac{T_1U^{(1)}(z_0)}{-2ik}\left(\frac{1}{\rho_2}\frac{\partial D^{(2)}}{\partial z}\right)(d^-). \end{aligned}$$

These equations yield

$$R_2 = \frac{\begin{vmatrix} D^{(1)}(d^+) & D^{(2)}(d^-) \\ \left(\frac{1}{\rho_1}\frac{\partial D^{(1)}}{\partial z}\right)(d^+) & \left(\frac{1}{\rho_2}\frac{\partial D^{(2)}}{\partial z}\right)(d^-) \end{vmatrix}}{\begin{vmatrix} U^{(1)}(d^+) & -D^{(2)}(d^-) \\ \left(\frac{1}{\rho_1}\frac{\partial U^{(1)}}{\partial z}\right)(d^+) & -\left(\frac{1}{\rho_2}\frac{\partial D^{(2)}}{\partial z}\right)(d^-) \end{vmatrix}},$$

$$T_1 = \frac{\begin{vmatrix} U^{(1)}(d^+) & -D^{(1)}(d^+) \\ \left(\frac{1}{\rho_1}\frac{\partial U^{(1)}}{\partial z}\right)(d^+) & -\left(\frac{1}{\rho_1}\frac{\partial D^{(1)}}{\partial z}\right)(d^+) \end{vmatrix}}{\begin{vmatrix} U^{(1)}(d^+) & -D^{(2)}(d^-) \\ \left(\frac{1}{\rho_1}\frac{\partial U^{(1)}}{\partial z}\right)(d^+) & -\left(\frac{1}{\rho_2}\frac{\partial D^{(2)}}{\partial z}\right)(d^-) \end{vmatrix}}.$$

We conclude that $\tilde{\psi}_1$ is given by

$$\tilde{\psi}_1(ka,z) = \begin{cases} \dfrac{R_1}{-2ik}D^{(1)}(z_0)D^{(1)}(z) - \dfrac{R_2}{2ik}U^{(1)}(z_0)U^{(1)}(z), & d < z < 0, \\ \dfrac{T_1}{-2ik}U^{(1)}(z_0)D^{(2)}(z) & , \quad h < z < d. \end{cases} \tag{14}$$

For $\tilde{\psi}_2$, as is shown in Figures 2(a) and 2(b), there are only four possi-

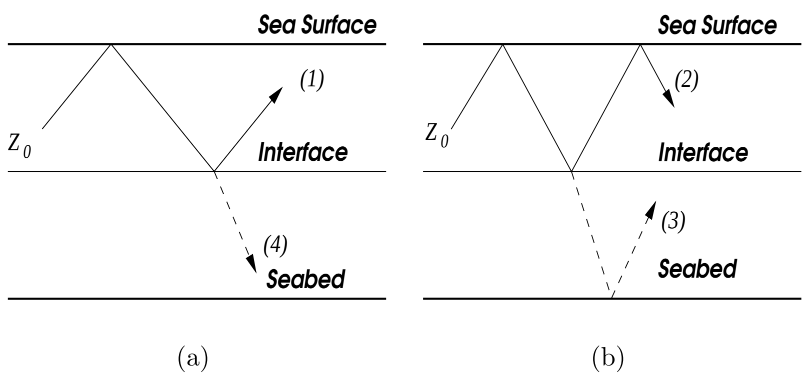

FIGURE 2. Schematic construction of $\tilde{\psi}_2$

bilities. For cases (1) and (4), by a similar argument as before, we write this up-going wave as $R_{21}D^{(1)}(z_0)U^{(1)}(z)/(-2ik)$ and the down-going wave as $T_{24}D^{(1)}(z_0)D^{(2)}(z)/(-2ik)$. To compute R_{21} and T_{24}, we use the transmission conditions to obtain the system

$$U^{(1)}(d^+)R_{21} - D^{(2)}(d^-)T_{24} = -R_1 D^{(1)}(d^+),$$

$$\left(\frac{1}{\rho_1}\frac{\partial U^{(1)}}{\partial z}\right)(d^+)R_{21} - \left(\frac{1}{\rho_2}\frac{\partial D^{(2)}}{\partial z}\right)(d^-)T_{24} = -R_1\left(\frac{1}{\rho_1}\frac{\partial D^{(1)}}{\partial z}\right)(d^+).$$

The above system implies

$$R_{21} = R_1 R_2, \tag{15}$$

$$T_{24} = R_1 T_1. \tag{16}$$

For case (2) in Figure 2(b), denoting this down-going wave by $R_{22}U^{(1)}(z_0) \times D^{(1)}(z)/(-2ik)$ and considering the pressure-release condition (9) lead to

$$\frac{R_2 U^{(1)}(z_0) U^{(1)}(0)}{-2ik} + \frac{R_{22} U^{(1)}(z_0) D^{(1)}(0)}{-2ik} = 0,$$

that is,

$$R_{22} = -R_2 \frac{U^{(1)}(0)}{D^{(1)}(0)} = R_1 R_2. \tag{17}$$

We denote the wave for case (3) in Figure 2(b) by $R_{23}U^{(1)}(z_0)U^{(2)}\partial z$. Since in the calculation of $\tilde{\psi}_1$, the incident wave for (3) has already been found to be $T_1 U^{(1)}(z_0) D^{(2)}(z)/(-2ik)$, we use the boundary condition (12) at $z = h$ to get

$$T_1 U^{(1)}(z_0) \frac{\partial D^{(2)}}{\partial z}(h^+) + R_{23} U^{(1)}(z_0) \frac{\partial U^{(2)}}{\partial z}(h^+) = 0. \tag{18}$$

Define B as

$$B := -\frac{\frac{\partial D^{(2)}}{\partial z}(h^+)}{\frac{\partial U^{(2)}}{\partial z}(h^+)}, \tag{19}$$

then R_{23} from (18) can be written as

$$R_{23} = B T_1. \tag{20}$$

Combining the results, $\tilde{\psi}_2$ is given by

$$\tilde{\psi}_2(ka, z) = \begin{cases} \dfrac{R_1 R_2}{-2ik} D^{(1)}(z_0) U^{(1)}(z) + \dfrac{R_1 R_2}{-2ik} U^{(1)}(z_0) D^{(1)}(z), & d < z < 0, \\ \dfrac{R_1 T_1}{-2ik} D^{(1)}(z_0) D^{(2)}(z) + \dfrac{T_1 B}{-2ik} U^{(1)}(z_0) U^{(2)}(z)\ , & h < z < d. \end{cases}$$

To construct $\tilde{\psi}_3$, we consider all the six possible cases as shown in Figure 3(a), 3(b) and 3(c). The up-going wave (6) represented by $T_{36}U^{(1)}(z_0)U^{(1)}(z)/(-2ik)$ and the down-going wave (5) represented by $R_{35}U^{(1)}(z_0)D^{(2)}(z)/(-2ik)$ can be determined by applying the transmission conditions to get

$$T_{36} = T_1 B T_2,$$
$$R_{35} = T_1 B R_5.$$

Here T_2 and R_5 are given by

$$T_2 := \frac{\begin{vmatrix} U^{(2)}(d^-) & -D^{(2)}(d^-) \\ \left(\frac{1}{\rho_2}\frac{\partial U^{(2)}}{\partial z}\right)(d^-) & -\left(\frac{1}{\rho_2}\frac{\partial D^{(2)}}{\partial z}\right)(d^-) \end{vmatrix}}{\begin{vmatrix} U^{(1)}(d^+) & -D^{(2)}(d^-) \\ \left(\frac{1}{\rho_1}\frac{\partial U^{(1)}}{\partial z}\right)(d^+) & -\left(\frac{1}{\rho_2}\frac{\partial D^{(2)}}{\partial z}\right)(d^-) \end{vmatrix}},$$

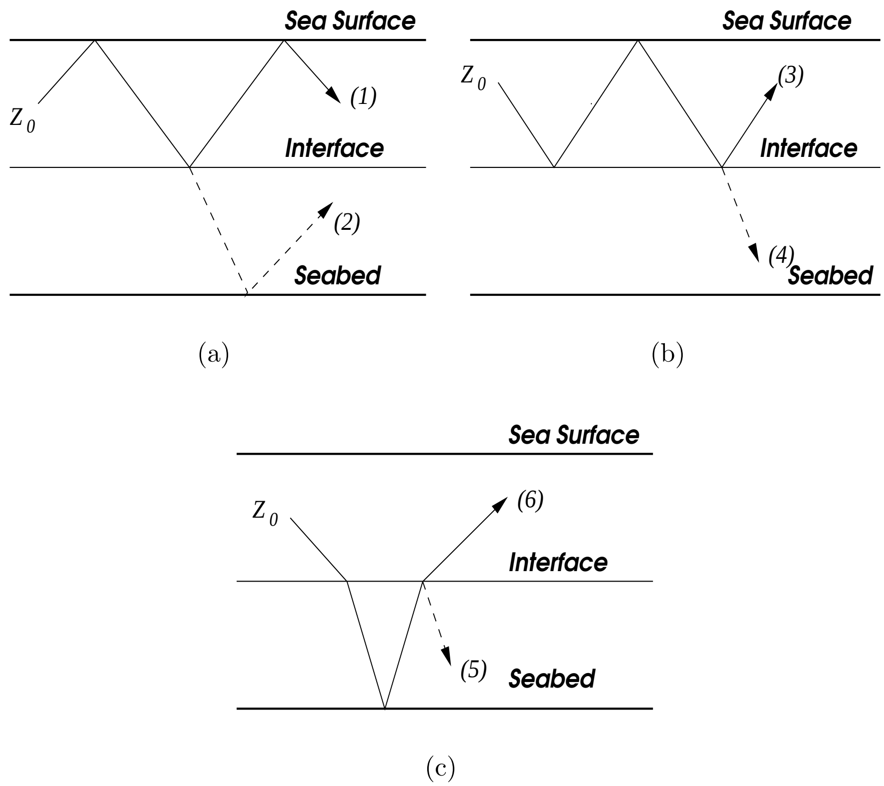

FIGURE 3. Schematic construction of $\tilde{\psi}_3$

$$R_5 := \frac{\begin{vmatrix} U^{(1)}(d^+) & U^{(2)}(d^-) \\ \left(\frac{1}{\rho_1}\frac{\partial U^{(1)}}{\partial z}\right)(d^+) & \left(\frac{1}{\rho_2}\frac{\partial U^{(2)}}{\partial z}\right)(d^-) \end{vmatrix}}{\begin{vmatrix} U^{(1)}(d^+) & -D^{(2)}(d^-) \\ \left(\frac{1}{\rho_1}\frac{\partial U^{(1)}}{\partial z}\right)(d^+) & -\left(\frac{1}{\rho_2}\frac{\partial D^{(2)}}{\partial z}\right)(d^-) \end{vmatrix}}.$$

Applying similar arguments to case (1) to (4) in Figures 3(a) and 3(b), we obtain the following representation of each individual wave:

$$\begin{aligned}
\text{Wave (1)}: &\ \frac{R_1^2 R_2}{-2ik}\, D^{(1)}(z_0) D^{(1)}(z),\\
\text{Wave (2)}: &\ \frac{R_1 T_1 B}{-2ik}\, D^{(1)}(z_0) U^{(2)}(z),\\
\text{Wave (3)}: &\ \frac{R_1 R_2^2}{-2ik}\, U^{(1)}(z_0) U^{(1)}(z),\\
\text{Wave (4)}: &\ \frac{R_1 R_2 T_1}{-2ik}\, U^{(1)}(z_0) D^{(2)}(z).
\end{aligned}$$

Using these six waves, $\tilde{\psi}_3$ is represented as

$$\tilde{\psi}_3(ka, z)$$

$$= \begin{cases} \frac{R_1^2 R_2}{-2ik} D^{(1)}(z_0) D^{(1)}(z) + \frac{R_1 R_2^2}{-2ik} U^{(1)}(z_0) U^{(1)}(z) + \frac{T_1 B T_2}{-2ik} U^{(1)}(z_0) U^{(1)}(z), \\ d < z < 0 \\ \frac{R_1 T_1 B}{-2ik} D^{(1)}(z_0) U^{(2)}(z) + \frac{R_1 R_2 T_1}{-2ik} U^{(1)}(z_0) D^{(2)}(z) + \frac{T_1 B R_5}{-2ik} U^{(1)}(z_0) D^{(2)}(z), \\ h < z < d. \end{cases}$$

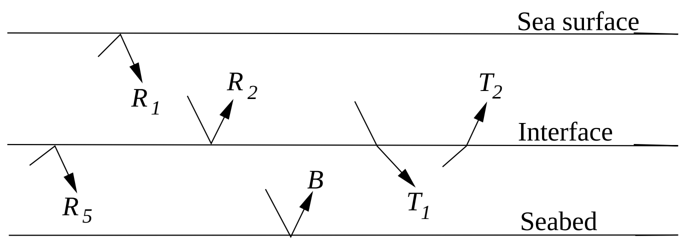

FIGURE 4. Schematic description of the six coefficients in the two-layer waveguide

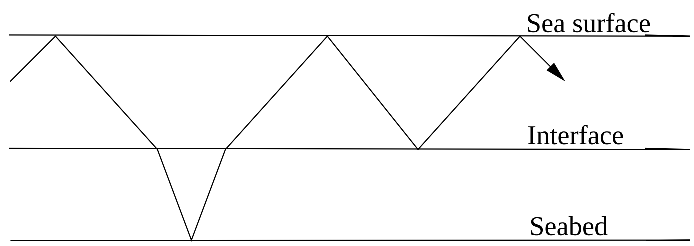

FIGURE 5. Schematic description of one of the rays in $\tilde{\psi}_7$. It can be represented by using the six parameters as $R_1 T_1 B T_3 R_1 R_2 R_1 D^{(1)}(z_0) D^{(2)}(z)/(-2ik)$

By induction, it can be shown that any possible wave can be uniquely represented in terms of the six coefficients R_1, R_2, R_5, T_1, T_2 and B defined as before. A schematic description of these 6 numbers is given in Figure 4. For example, the down-going wave in Figure 5 is $R_1 T_1 B T_3 R_1 R_2 R_1 D^{(1)}(z_0) D^{(2)}(z)/(-2ik)$. Therefore we may construct $\tilde{\psi}_n$, $n = 1, 2, 3, \ldots$ by the following scheme based on a tree structure. The tree structure is built by the four rules:

(1) R_1 always branches out to T_1 and R_2 in the next level of the tree.
(2) T_1 can only be followed by B. R_2 can only be followed by R_1.
(3) B always branches into T_2 and R_5 in the next level.
(4) T_2 can only be followed by R_1. R_5 can only be followed by B.

We divide the waves in ψ_n, $n > 1$ into two groups: one group includes all the waves which have $D^{(1)}(z_0)$ as part of the coefficients and the other group includes all the waves involving $U^{(1)}(z_0)$. For the first group, the root of the tree is R_1 and the tree is shown in Figure 6(a). The other group contains two trees – one starts with R_2 and the other starts with T_1. These two trees are shown in Figure 6(b). Using these tree structures, ψ_n, $n \geq 1$, can be constructed by tracing **every** path from the root (level 1) to the nodes at level n. For example, the length-four path R_1-T_1-B-T_2 of Tree (a) corresponds to the wave $\frac{R_1T_1BT_2}{-2ik}D^{(1)}(z_0)U^{(1)}(z)$. After all paths of length n in all the three trees are traced, $\psi_n(z)$ in $d < z < 0$ is then given by the sum of all waves which contain $U^{(1)}(z)$ or $D^{(1)}(z)$, and $\psi_n(z)$ in $h < z < d$ is given by the sum of all waves which contain $U^{(2)}(z)$ or $D^{(2)}(z)$.

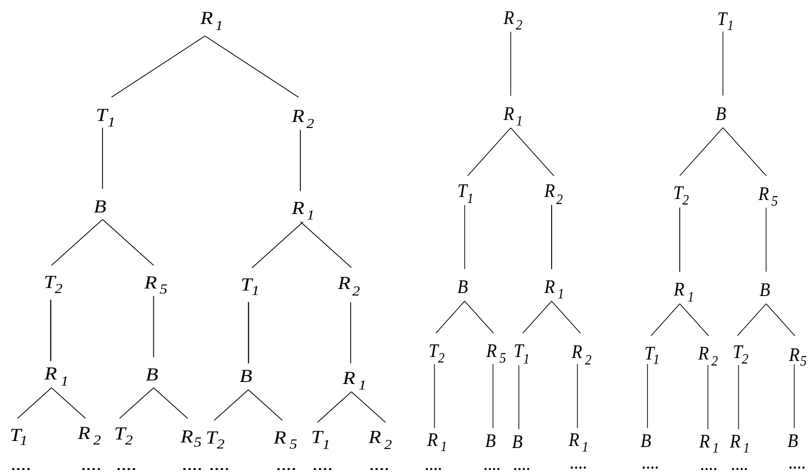

(a) (b)

Figure 6. Tree Structure

The ray representation is then obtained by inverse Hankel transforming $\sum_{l=0}^{\infty}\tilde{\psi}_l$ back.

3. Relation Between the Multiple Scattering Representation and the Hankel Transformed Representation of the Green's Function

The multiple scattering representation constructed in the previous section can actually be derived in a simpler way by using binomial expansions as presented in this section.

It is known that the Green's function for the system of (7)–(12) can be constructed by using two functions $\tilde{f}_1$ and $\tilde{f}_2$ such that both of them satisfy the differential equations (7), (8) and the transmission conditions (10). Furthermore, $\tilde{f}_1$ satisfies the boundary condition (9), whereas $\tilde{f}_2$ satisfies the boundary condition (12). Because $\{U^{(1)}, D^{(1)}\}$ and $\{U^{(2)}, D^{(2)}\}$ are linearly independent solutions of (7) and (8), respectively, we can write $\tilde{f}_1$ and $\tilde{f}_2$ as

$$\tilde{f}_1 = \begin{cases} U^{(1)} + R_1D^{(1)}, & d < z < 0, \\ \alpha U^{(2)} + \beta D^{(2)}, & h < z < d, \end{cases}$$

$$\tilde{f}_2 = \begin{cases} \gamma U^{(1)} + \delta D^{(1)}, & d < z < 0, \\ D^{(2)} + BU^{(2)}, & h < z < d. \end{cases}$$

Here R_1 and B are defined as in (13) and (19). To determine the constants, we apply the transmission conditions (10) and (11) to obtain

$$\alpha = \frac{\begin{vmatrix} U^{(1)}(d^+) & D^{(2)}(d^-) \\ \left(\frac{1}{\rho_1}\frac{\partial U^{(1)}}{\partial z}\right)(d^+) & \left(\frac{1}{\rho_2}\frac{\partial D^{(2)}}{\partial z}\right)(d^-) \end{vmatrix} + R_1 \begin{vmatrix} D^{(1)}(d^+) & D^{(2)}(d^-) \\ \left(\frac{1}{\rho_1}\frac{\partial D^{(1)}}{\partial z}\right)(d^+) & \left(\frac{1}{\rho_2}\frac{\partial D^{(2)}}{\partial z}\right)(d^-) \end{vmatrix}}{\begin{vmatrix} U^{(2)}(d^-) & D^{(2)}(d^-) \\ \left(\frac{1}{\rho_2}\frac{\partial U^{(2)}}{\partial z}\right)(d^-) & \left(\frac{1}{\rho_2}\frac{\partial D^{(2)}}{\partial z}\right)(d^-) \end{vmatrix}}$$

$$\beta = \frac{\begin{vmatrix} U^{(1)}(d^+) & D^{(2)}(d^-) \\ \left(\frac{1}{\rho_1}\frac{\partial U^{(1)}}{\partial z}\right)(d^+) & \left(\frac{1}{\rho_2}\frac{\partial D^{(2)}}{\partial z}\right)(d^-) \end{vmatrix} + R_1 \begin{vmatrix} D^{(1)}(d^+) & D^{(2)}(d^-) \\ \left(\frac{1}{\rho_1}\frac{\partial D^{(1)}}{\partial z}\right)(d^+) & \left(\frac{1}{\rho_2}\frac{\partial D^{(2)}}{\partial z}\right)(d^-) \end{vmatrix}}{\begin{vmatrix} U^{(2)}(d^-) & D^{(2)}(d^-) \\ \left(\frac{1}{\rho_2}\frac{\partial U^{(2)}}{\partial z}\right)(d^-) & \left(\frac{1}{\rho_2}\frac{\partial D^{(2)}}{\partial z}\right)(d^-) \end{vmatrix}}$$

$$\gamma = \frac{-\begin{vmatrix} D^{(1)}(d^+) & D^{(2)}(d^-) \\ \left(\frac{1}{\rho_1}\frac{\partial D^{(1)}}{\partial z}\right)(d^+) & \left(\frac{1}{\rho_2}\frac{\partial D^{(2)}}{\partial z}\right)(d^-) \end{vmatrix} + B \begin{vmatrix} D^{(1)}(d^+) & D^{(2)}(d^-) \\ \left(\frac{1}{\rho_1}\frac{\partial D^{(1)}}{\partial z}\right)(d^+) & \left(\frac{1}{\rho_2}\frac{\partial D^{(2)}}{\partial z}\right)(d^-) \end{vmatrix}}{\begin{vmatrix} U^{(1)}(d^+) & D^{(1)}(d^+) \\ \left(\frac{1}{\rho_1}\frac{\partial U^{(1)}}{\partial z}\right)(d^+) & \left(\frac{1}{\rho_1}\frac{\partial D^{(1)}}{\partial z}\right)(d^+) \end{vmatrix}}$$

$$\delta = \frac{\begin{vmatrix} U^{(1)}(d^+) & D^{(2)}(d^-) \\ \left(\frac{1}{\rho_1}\frac{\partial U^{(1)}}{\partial z}\right)(d^+) & \left(\frac{1}{\rho_2}\frac{\partial D^{(2)}}{\partial z}\right)(d^-) \end{vmatrix} - B \begin{vmatrix} U^{(1)}(d^+) & D^{(2)}(d^-) \\ \left(\frac{1}{\rho_1}\frac{\partial U^{(1)}}{\partial z}\right)(d^+) & \left(\frac{1}{\rho_2}\frac{\partial D^{(2)}}{\partial z}\right)(d^-) \end{vmatrix}}{\begin{vmatrix} U^{(1)}(d^+) & D^{(1)}(d^+) \\ \left(\frac{1}{\rho_1}\frac{\partial U^{(1)}}{\partial z}\right)(d^+) & \left(\frac{1}{\rho_1}\frac{\partial D^{(1)}}{\partial z}\right)(d^+) \end{vmatrix}}$$

In terms of $\tilde{f}_1$ and $\tilde{f}_2$, the Green's function $\tilde{G}(z, z_0)$ is

$$\tilde{G}(z, z_0) = \frac{\tilde{f}_1(z_>)\tilde{f}_1(z_<)}{W(\tilde{f}_1, \tilde{f}_2)(z_0)},$$

where $W(\tilde{f}_1, \tilde{f}_2)(z_0)$ is the Wronskian of $\tilde{f}_1$ and $\tilde{f}_2$ evaluated at $z = z_0$. Therefore, for z_0 in the ocean layer, i.e., for $d < z_0 < 0$, we have

$$\begin{aligned} &\tilde{G}(z, z_0) \\ &= \begin{cases} \dfrac{[U^{(1)}(z_>) + R_1 D^{(1)}(z_>)] \cdot [\frac{\gamma}{\delta} U^{(1)}(z_<) + D^{(1)}(z_<)]}{-2ik(1 - R_1 \cdot \frac{\gamma}{\delta})}, & d < z < 0, \\ \dfrac{\frac{1}{\delta} \cdot [U^{(1)}(z_0) + R_1 D^{(1)}(z_0)][D^{(2)}(z) + BU^{(2)}(z)]}{-2ik(1 - R_1 \cdot \frac{\gamma}{\delta})}, & h < z < d. \end{cases} \end{aligned} \tag{21}$$

The key step in connecting the above expression of the Green's function with the multiple scattering representation in $d < z < 0$ is to identify $\frac{\gamma}{\delta}$ with the following combination of the parameters listed in Figure 4:

$$\frac{\gamma}{\delta} = R_2 + \frac{BT_1T_2}{1 - BR_5}. \tag{22}$$

Applying the binomial expansion to the first function in (21), the coefficient of the term $U^{(1)}(z_>)D^{(1)}(z_<)$ becomes

$$\frac{1}{-2ik} + \sum_{k=1}^{\infty}\sum_{l=0}^{k} \frac{C_l^k (R_2R_1)^l}{-2ik}\left(\sum_{j=0}^{\infty} T_1(BR_5)^j BT_2R_1\right)^{k-l}, \tag{23}$$

$$C_l^k := \frac{k!}{(k-l)!\,l!}. \tag{24}$$

Similarly, the coefficient of $U^{(1)}(z_>)U^{(1)}(z_<)$ in (21) is

$$\begin{aligned}
&\frac{R_2}{-2ik} + \sum_{j=0}^{\infty}\frac{T_1B(R_5B)^jT_2}{-2ik}\\
&+ \sum_{k=1}^{\infty}\sum_{l=0}^{k} \frac{C_l^k (R_2R_1)^l}{-2ik}\left(\sum_{m=0}^{\infty} T_1(BR_5)^m BT_1T_2\right)^{k-l} \sum_{j=0}^{\infty} T_1B(R_5B)^jT_2\\
&+ \sum_{k=1}^{\infty}\sum_{l=0}^{k} \frac{C_l^k (R_2R_1)^l}{-2ik}\left(\sum_{m=0}^{\infty} T_1(BR_5)^m BT_1T_2\right)^{k-l} R_2,
\end{aligned} \tag{25}$$

and the coefficient of $D^{(1)}(z_>)D^{(1)}(z_<)$ is

$$\frac{R_1}{-2ik} + \frac{R_1}{-2ik}\sum_{k=1}^{\infty}\sum_{l=0}^{k} C_l^k (R_2R_1)^l\left(\sum_{j=0}^{\infty} T_1(BR_5)^j BT_2R_1\right)^{k-l}. \tag{26}$$

Finally, the coefficient of $D^{(1)}(z_>)U^{(1)}(z_<)$ is

$$\sum_{k=1}^{\infty}\sum_{l=0}^{k} \frac{C_l^k (R_2R_1)^l}{-2ik}\left(\sum_{j=0}^{\infty} T_1(BR_5)^j BT_2R_1\right)^{k-l}. \tag{27}$$

For the Green's function in $h < z < d$, applying (22) and the identity

$$\frac{1}{\delta} = \frac{T_1}{1 - BR_5},$$

followed by binomial expansions, we obtain the series expansion of the coefficient of the term $U^{(1)}(z_0)U^{(2)}(z)$ of the Green's function $G(z, z_0)$ in $h < z < d$:

$$\frac{1}{-2ik}\sum_{k=0}^{\infty}\sum_{l=0}^{k} C_l^k (R_2R_1)^l T_1B\left[T_2R_1T_1B\sum_{n=0}^{\infty}(R_5B)^n\right]^{k-l}\sum_{m=0}^{\infty}(R_5B)^m. \tag{28}$$

In a similar fashion, the coefficient of the term $U^{(1)}(z_0)D^{(2)}(z)$ can be written as

$$\frac{1}{-2ik}\sum_{k=0}^{\infty}\sum_{l=0}^{k}C_l^k(R_2R_1)^lT_1\left[BT_2R_1T_1\sum_{n=0}^{\infty}(BR_5)^n\right]^{k-l}\sum_{m=0}^{\infty}(BR_5)^m, \qquad (29)$$

and for $D^{(1)}(z_0)U^{(2)}(z)$ we have

$$\frac{R_1}{-2ik}\sum_{k=0}^{\infty}\sum_{l=0}^{k}C_l^k(R_2R_1)^lT_1\left[BT_2R_1T_1\sum_{n=0}^{\infty}(BR_5)^n\right]^{k-l}\sum_{m=0}^{\infty}(BR_5)^m\cdot B. \qquad (30)$$

Finally, the coefficient of the term $D^{(1)}(z_0)D^{(2)}(z)$ can be expressed as

$$\frac{R_1}{-2ik}\sum_{k=0}^{\infty}\sum_{l=0}^{k}C_l^k(R_2R_1)^lT_1\left[BT_2R_1T_1\sum_{n=0}^{\infty}(BR_5)^n\right]^{k-l}\sum_{m=0}^{\infty}(BR_5)^m. \qquad (31)$$

Clearly, there is a one-to-one correspondence between each of the terms in these expansions and the waves constructed by using the tree structures in Figures 6(a) and 6(b).

References

1. D. S. Ahluwalia and J. B. Keller, Exact and asymptotic representations of the sound field in a stratified ocean. *Wave propagation and underwater acoustics* (*Workshop, Mystic, Conn.,* 1974), 14–85. *Lecture Notes in Phys.,* Vol. 70, *Springer, Berlin,* 1977.
2. S. Bergman and M. Schiffer, Kernel functions and elliptic differential equations in mathematical physics. *Academic Press Inc., New York, N. Y.,* 1953.
3. R. P. Gilbert, C. Mawata, and Y. Xu, Determination of a distributed inhomogeneity in a two-layered waveguide from scattered sound. *Direct and inverse problems of mathematical physics* (*Newark, DE,* 1997), 107–124, *Int. Soc. Anal. Appl. Comput.,* 5, *Kluwer Acad. Publ., Dordrecht,* 2000.
4. R. P. Gilbert and M.-J. Ou, A uniqueness theorem of the 3-dimensional acoustic scattering problem in a shallow ocean with a fluid-like seabed. *J. Comput. Acoust.* **11**(2003), No. 4, 535–549.
5. R. P. Gilbert and Y. Xu, An inverse problem for harmonic acoustics in stratified oceans. *J. Math. Anal. Appl.* **176**(1993), No. 1, 121–137.
6. C. Rozier, D. Lesselier, T. S. Angell, and R. E. Kleinman, Reconstruction of an impenetrable obstacle immersed in a shallow water acoustic waveguide. *Inverse problems of wave propagation and diffraction* (*Aix-les-Bains,* 1996), 130–142, *Lecture Notes in Phys.,* 486, *Springer, Berlin,* 1997.
7. C. Rozier, D. Lesselier, T. S. Angell, and R. E. Kleinman, Shape retrieval of an obstacle immersed in shallow water from single-frequency farfields using a complete family method. *Inverse Problems* **13**(1997), No. 2, 487–508.

(Received 25.04.2006)

Authors' addresses:

R. Gilbert

Department of Mathematical Sciences
University of Delaware
Newark, Delaware 19716
USA

Miao-Jung Ou
Department of Mathematics
University of Central Florida
Orlando, FL 32816
USA
E-mail: mou@mail.ucf.edu